Resonant guided elastic waves in an adsorbed bilayer: Theoretical analysis of the density of states

E. H. El Boudouti
Laboratoire de Dynamique et Structure des Matériaux Moléculaires, Centre National de la Recherche Scientifique, Unité de Physique, Université de Lille I, 59655 Villeneuve d'Ascq Cedex, France
and Département de Physique, Faculté des Sciences, Oujda, Morocco

B. Djafari-Rouhani and A. Akjouj*
Laboratoire de Dynamique et Structure des Matériaux Moléculaires, Centre National de la Recherche Scientifique, Unité de Physique, Université de Lille I, 59655 Villeneuve d'Ascq Cedex, France

(Received 6 September 1996; revised manuscript received 11 October 1996)

We study resonant acoustic waves of sagittal polarization in a bilayer deposited on a substrate. Such resonances were initially studied by Brillouin light scattering in a buffer silica layer of a Si-SiO_2 bilayer on a Si substrate. Using a Green's-function method, we have obtained the local and total densities of states as a function of the frequency ω and the wave vector $\mathbf{k}_\parallel$ parallel to the interfaces. When the velocities of sound in the buffer layer are higher than those in the topmost layer the former acts as a barrier between phonons of the topmost layer and those of the substrate; therefore well-confined resonant waves may exist in the higher slab, which appear as well-defined peaks in the density of states. The positions of these peaks enable us to study the speed of resonant modes as a function of the parallel wave vector and the thicknesses of the buffer and topmost layers. Specific applications of our analytical results are given in this paper for a GaAs-Si bilayer on a GaAs substrate.

I. INTRODUCTION

The propagation of surface acoustic waves in adsorbed layers, the so-called Love[1] and Sezawa and Kanai[2] modes, has been extensively studied since the beginning of this century. These modes[3] are respectively of shear horizontal and sagittal polarizations, which means a polarization perpendicular or parallel to the sagittal plane defined by the normal to the surface and the wave vector $\mathbf{k}_\parallel$ parallel to the surface. These studies[4–12] have been performed mostly in the vicinity of the transverse threshold of adsorbate layers and below the transverse velocity of sound in the substrate and therefore these modes become guided waves of transverse character in adsorbed layers.

Some years ago,[13–21] much attention has been devoted to the propagation of acoustic modes lying above the substrate velocity of sound and at the vicinity of the longitudinal threshold of the adsorbate, the so-called longitudinal guided modes (LGM's). The LGM's are resonances (also called leaky or pseudowaves) with a displacement field having longitudinal character and propagating in the film. These pseudomodes are of sagittal polarization and are without analogy in the case of shear horizontal polarization. LGM's in one adsorbed layer[14–17] were investigated by Brillouin light scattering, and the experimental results were found to be in agreement with a Brillouin scattering cross-section theory.[16]

Some very recent papers[19,20] gave experimental evidence and theoretical explanation of Brillouin light scattering from sagittal surface acoustic phonons in a structure composed of a Si-SiO_2 double layer on a Si substrate. The main features in this system are related to the buried SiO_2 layer. The $p \cdot p$ Brillouin spectra show, in addition to the usual sagittal modes (Rayleigh and Sezawa waves), two longitudinal guided pseudomodes near the longitudinal threshold of Si that are analogous to those previously observed in a single adsorbed layer.[14–16] Similar investigations were performed on a silicon-oxynitride-fused-silica (Si-SiON) double layer deposited onto a Si substrate[13] and on Zn_nSe-$Z_nSe_{1-x}S_x$ strained layer superlattices.[22] The measure of surface modes and pseudomodes by Brillouin spectroscopy helps one to characterize the elastic properties of thin films[17,21] and superlattices.[4–9,22]

Among different mathematical approaches, the Green's-function method is quite suitable for studying the spectral properties of these composite materials; in particular, it enables us to calculate the total or local density of states (DOS) in which the localized or resonant surface modes appear as well-defined peaks. We have previously[18] applied such a formalism to the case of one adsorbed layer. In the present paper we are interested in calculating both local and total DOS associated with the more complicated case of sagittal acoustic modes in an adsorbed bilayer. The knowledge of the DOS in these structures enables us to determine the spatial distribution of the modes and in particular the possibility of guided pseudomodes, which may appear as well-defined peaks of the DOS in the continuum of the substrate bulk band. The Green's-function approach used in this work is also of interest for the calculation of transmission and reflection coefficients,[23,24] or for studying the scattering of light by surface phonons.[25]

Our analytical results can of course be applied to any

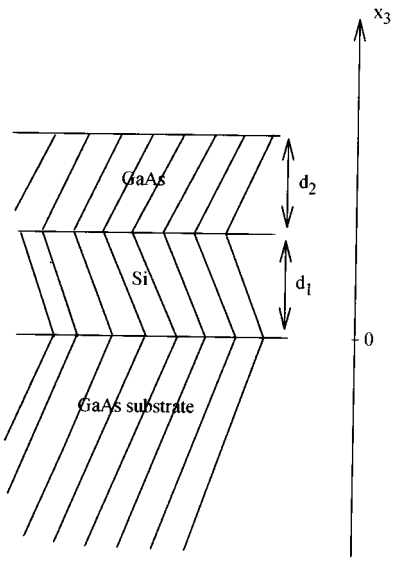

FIG. 1. Schematic representation of a bilayer deposited on a homogeneous substrate. d_1 and d_2 are, respectively, the thickness of the buffer and of the surface layer.

combination of material parameters in the bilayer and in the substrate. In this paper we shall focus our attention on a phenomenon that apparently has not been discussed in previous works: this is the possibility of finding well-defined guided pseudomodes in the topmost layer, as a consequence of its separation from the substrate by the buffer layer, when the velocities of sound in the buffer are higher than those in the topmost layer. This phenomenon results from the fact that some of the slab modes of the top layer, even if they are in resonance with the substrate bulk modes, cannot propagate in the intermediate layer and therefore remain well-defined guided waves of the higher slab. A preliminary report of these results[26] as well as the results associated with the simplest case of transverse polarization[27] were presented elsewhere.

After a brief presentation of the model in Sec. II, we give in Sec. III some numerical results for a GaAs-Si bilayer deposited on GaAs.

II. MODEL

The adsorbed bilayer is formed out of two different slabs ($i=1,2$) deposited on a homogeneous substrate $i=s$. The slabs are respectively of thickness d_1 and d_2. All the interfaces are taken to be parallel to the (x_1,x_2) plane. A space position along the x_3 axis in medium i is indicated by (i,x_3), where $-d_i/2 \leqslant x_3 \leqslant d_i/2$ in the two adsorbed layers and $x_3 \leqslant 0$ in the substrate (see Fig. 1).

The media forming the slabs and the substrate are assumed to be isotropic elastic media characterized by their mass densities ρ and their elastic constants C_{11} and C_{44}. The squares of the bulk longitudinal and shear plane wave velocities are, respectively,

$$C_l^2=\frac{C_{11}}{\rho}, \quad C_t^2=\frac{C_{44}}{\rho}. \tag{1}$$

Due to the isotropy within the (x_1,x_2) plane, the shear horizontal vibrations are decoupled from those polarized within the sagittal plane, for any value of the propagation vector $k_\parallel$ parallel to the surface.

We obtain the local and total DOS associated with the supported double layers from the knowledge of the corresponding Green's function, which is calculated here by using the theory of interface response in composite materials.[23] In this theory, the Green function $\mathbf{g}$ of a composite system can be written as[23]

$$\mathbf{g}(DD)=\mathbf{G}(DD)+\mathbf{G}(DM)[\mathbf{G}^{-1}(MM)\mathbf{g}(MM)\mathbf{G}^{-1}(MM) - \mathbf{G}^{-1}(MM)]\mathbf{G}(MD), \tag{2}$$

where D and M are, respectively, the whole space and the space of the interfaces in the composite material. Within an elastic model, M is just limited to the planes $x_3=0\equiv -d_1/2, d_1/2\equiv -d_2/2$ and $d_2/2$ (see Fig. 1). $\mathbf{G}$ is a block-diagonal matrix in which each block $\mathbf{G}_i$ corresponds to the bulk Green function of the subsystem i. In our case, the composite material is composed of slabs of materials i ($i=1,2$) with thickness d_i deposited on a substrate of material $i=s$. In Eq. (2) the calculation of $\mathbf{g}(DD)$ requires, besides $\mathbf{G}_i$, the knowledge of $\mathbf{g}(MM)$. In practice, the latter is obtained[23] by inverting the matrix $\mathbf{g}^{-1}(MM)$, which can be simply built from a juxtaposition of the matrices $\mathbf{g}_{si}^{-1}(MM)$, where $\mathbf{g}_{si}(MM)$ is the interface Green's function of the slabs i ($i=1,2$) and of the substrate alone. Let us emphasize that, in the geometry of the adsorbed bilayer, the elements of the Green's function take the form $g_{\alpha\beta}(\omega^2,k_\parallel|i,x_3;i',x_3')$, where ω is the frequency of the acoustic wave, $k_\parallel$ the wave vector parallel to the interfaces, and α,β denote the directions x_1 ($\equiv 1$), x_2 ($\equiv 2$), and x_3 ($\equiv 3$). For the sake of simplicity, we shall omit in the following the parameters ω^2 and $k_\parallel$, and we note as $\mathbf{g}(i,x_3;i',x_3')$ the 3×3 matrix whose elements are $g_{\alpha\beta}(i,x_3,i',x_3')$ ($\alpha,\beta=1,2,3$).

By assuming that $k_\parallel$ is along the x_1 direction, the components g_{22} of the Green function decouple from the components $g_{11},g_{13},g_{31},g_{33}$ (i.e., $g_{12}=g_{21}=g_{23}=g_{32}=0$); the former corresponds to shear horizontal vibrations, whereas the latter are associated with the vibrations polarized in the sagittal plane.

From the knowledge of the Green's function in the supported double layers, one obtains for a given value of $k_\parallel$ the local density of states

$$n_\alpha(\omega^2,k_\parallel;x_3)=-\frac{1}{\pi}\,\mathrm{Im}\, g_{\alpha\alpha}(\omega^2,k_\parallel|i,x_3;i,x_3) \quad (\alpha=1,2,3) \tag{3a}$$

or

$$n_\alpha(\omega,k_\parallel;x_3)=-\frac{2\omega}{\pi}\,\mathrm{Im}\, g_{\alpha\alpha}(\omega^2,k_\parallel|i,x_3;i,x_3) \quad (\alpha=1,2,3) \tag{3b}$$

The total density of states for a given value of $k_\parallel$ is obtained by integrating over x_3 the local density of state $n(\omega^2,k_\parallel;x_3)$ and by summing over the index α. This expression can be written as the sum of three contributions:

$$n(\omega^2)=n_1(\omega^2)+n_2(\omega^2)+n_s(\omega^2), \tag{4}$$

TABLE I. Transverse and longitudinal velocities and mass densities for GaAs and Si.

	C_t (m/s)	C_l (m/s)	ρ (kg/m^3)
GaAs	3342	4710	5316.9
Si	5845	8440	2330

where $n_1(\omega^2)$ and $n_2(\omega^2)$ are the contributions of layers 1 and 2, respectively, and $n_s(\omega^2)$ comes from the substrate. Actually, in the latter term, we subtract the contribution $n_B(\omega^2)$ of the bulk of the substrate, which is an infinite quantity and write $n_s(\omega^2)=n_B(\omega^2)+\Delta_s n(\omega^2)$.

Then we have

$$n_1(\omega^2)=-\frac{\rho^{(1)}}{\pi}\,\mathrm{Im\,tr}\int_{-d_1/2}^{d_1/2}\mathbf{g}(i=1,x_3;i=1,x_3)\,dx_3, \quad (5)$$

$$n_2(\omega^2)=-\frac{\rho^{(2)}}{\pi}\,\mathrm{Im\,tr}\int_{-d_2/2}^{d_2/2}\mathbf{g}(i=2,x_3;i=2,x_3)\,dx_3, \quad (6)$$

$$\Delta_s n(\omega^2)=-\frac{\rho^{(s)}}{\pi}\,\mathrm{Im\,tr}\int_{-\infty}^{0}[\mathbf{g}(i=s,x_3;i=s,x_3) - \mathbf{G}_s(x_3,x_3)]\,dx_3. \quad (7)$$

g and $\mathbf{G}_s$ are, respectively, the response functions of the adsorbed bilayer and of an infinite substrate. The trace is taken over the components 11 and 33, which contribute to the sagittal modes we are studying in this paper. The integration over x_3 can be performed very easily because the Green's-functions elements are only composed of exponential terms.[28]

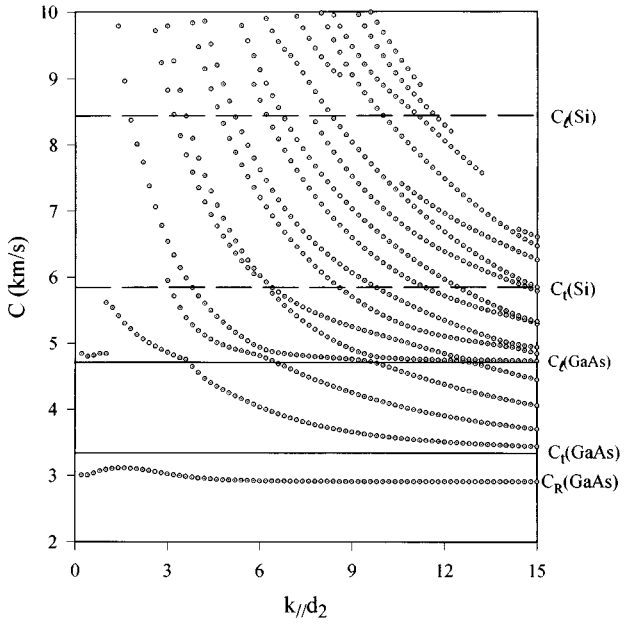

FIG. 2. Dispersion curves of resonant sagittal modes for a GaAs-Si bilayer on a GaAs substrate. C is the velocity. The figure is sketched for $d_1/d_2=0.5$, where d_1 and d_2 are, respectively, the thickness of the Si and GaAs slabs.

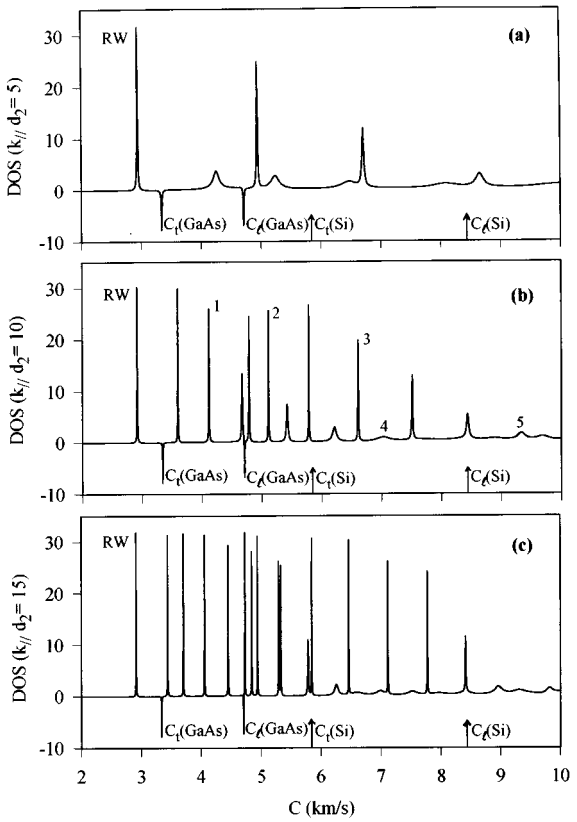

FIG. 3. Variation of the DOS due to the adsorption of the GaAs-Si bilayer on the GaAs substrate, at $k_\parallel d_2=5$ (a), 10 (b), and 15 (c). The antiresonances appearing at C_t(GaAs) and C_l(GaAs) correspond to δ peaks of weight $-\frac{1}{4}$, resulting from the subtraction of the substrate bulk band in the variation of the DOS [see Eq. (7)]. The arrows indicate the positions of the transverse and longitudinal velocities of Si.

To end this section, let us notice that, to the best of our knowledge, the supported double-layer Green's function associated with sagittal modes has not been calculated before.[28] The shear horizontal component of this Green's function was given recently.[12,27]

III. NUMERICAL RESULTS

This section contains a few illustrations of local and total densities of states and dispersion curves for sagittal acoustic waves in a GaAs-Si bilayer deposited on a GaAs substrate cut along the (001) plane and for propagation wave vector $\mathbf{k}_\parallel$ along the [100] direction (see Fig. 1). The parameters for the materials are listed in Table I. In this structure the velocities of sound in the Si buffer layer are higher than those in the GaAs topmost layer; therefore the former acts as a barrier between phonons of the topmost layer and those of the substrate, and well-confined resonant waves may exist in the higher slab in such a way as to realize an acoustic waveguide. Similar illustrations were presented for pure shear horizontal (SH) waves in a very recent paper.[27] In the case of sagittal acoustic waves studied here, we show that guided longitudinal acoustic waves with velocities lying in the range of longitudinal velocities of sound may be confined in the topmost layer.

Figure 2 gives an illustration of the dispersion curves (ve-

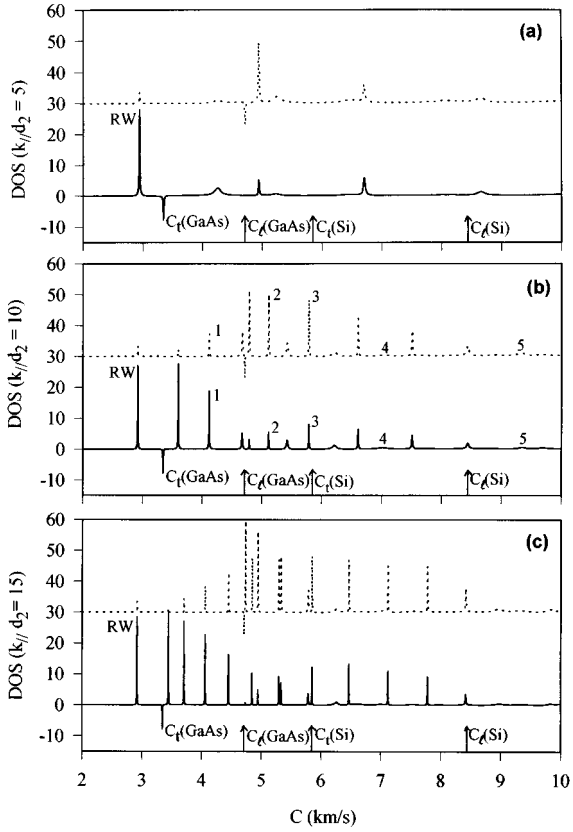

FIG. 4. Same as in Fig. 3, where the contributions of shear vertical (full curves) and of longitudinal (dashed curves) components in the DOS are separated.

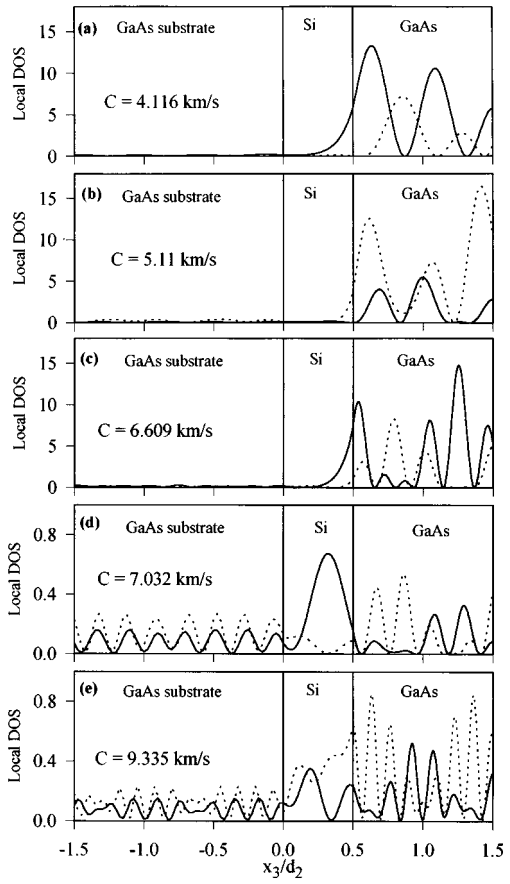

FIG. 5. Spatial representation of the local DOS for $C=4.116$ km/s, 5.11 km/s, 6.609 km/s, 7.032 km/s, and 9.335 km/s at $k_{\|}d_2=10$. These pseudomodes are, respectively, labeled 1, 2, 3, 4, and 5 in Fig. 3(b). The full (dashed) curves correspond to shear-vertical (longitudinal) components of the local DOS. The space positions of the different interfaces are marked by vertical lines.

locity C versus the reduced parallel wave vector $k_{\|}d_2$). The thickness d_1 of the Si slab is such that $d_1=0.5d_2$, where d_2 is the thickness of the GaAs layer (see Fig. 1). Apart the lowest branch corresponding to the Rayleigh wave (RW) localized at the surface of the GaAs layer, the other branches represent resonant modes induced by the bilayer in the continuum of the substrate bulk band, which means above the transverse velocity of sound of the GaAs substrate. These resonant modes are depicted from the maxima of the DOS, shown in Fig. 3 for a few values of the wave vector $k_{\|}d_2$. The full (dashed) horizontal lines in Fig. 2 represent the positions of transverse and longitudinal velocities of sound of GaAs (Si) medium. In the limit $k_{\|}d_2\rightarrow\infty$ in Fig. 2, the resonant modes move to the GaAs transverse sound line. The pseudomodes below C_t(Si) represent resonant guided waves of the topmost GaAs layer, and appear as well-defined peaks in the DOS of Fig. 3, even though they are in resonance with the bulk modes of the GaAs substrate. For the sake of illustration of very narrow peaks, these resonances are enlarged by adding a small imaginary part ϵ to the velocity C [$\epsilon=10^{-3}\times C_t$(GaAs)]. One can, however, notice that the widths of these peaks become large when either $k_{\|}d_2$ or the thickness d_1 of the buffer layer decreases (see below).

Among the above guided waves, one can distinguish the modes falling between C_t(GaAs) and C_l(GaAs), which are predominantly of shear vertical character and the branches falling between C_l(GaAs) and C_t(Si), which are predominantly of longitudinal character. This is shown in Fig. 4 where we have separated in the DOS the contributions of shear vertical (full curves) and of longitudinal (dashed curves) components. One can also notice in Fig. 2 important coupling and anticrossing of these pseudomodes in the vicinity of the GaAs longitudinal sound line. In Fig. 2 there are also well-defined resonances with velocities falling between C_t(Si) and C_l(Si), which are guided waves of the whole GaAs/Si bilayer. More specifically, as will be shown below, one can distinguish in this velocity range narrow and intense resonances that are associated with the GaAs topmost layer, separated by small and broad peaks corresponding to the Si buffer layer [see Figs. 3(b) and 3(c)]. These resonances have mixed shear vertical and longitudinal character as shown in Fig. 4. Above C_l(Si), the resonances become very weak especially for small values of $k_{\|}d_2$.

An analysis of the local DOS as a function of the space position x_3 (Fig. 5) clearly shows the localization properties of the different kinds of modes belonging to different velocity range. The local DOS reflects the spatial behavior of the square modulus of the displacement field. Figures 5(a) and 5(b) correspond to the modes respectively labeled 1 and 2 in Figs. 3(b) and 4(b), showing that these pseudomodes are confined in the GaAs slab and do not propagate into the Si buffer layer. Consequently, they remain well-defined guided waves of the topmost GaAs slab; however, the first one [Fig.

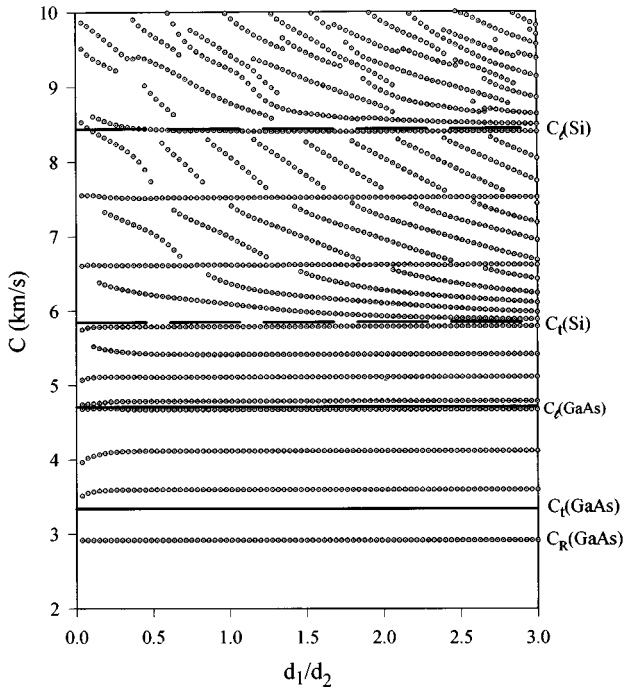

FIG. 6. Variation of the velocity of the resonant modes, for $k_{\parallel}d_2=10$, as a function of d_1/d_2.

5(a)] is predominately of shear vertical character as its velocity ($C=4.116$ km/s) lies between C_t(GaAs) and C_l(GaAs), while the second one [Fig. 5(b)] with a velocity $C=5.11$ km/s lying between C_l(GaAs) and C_t(Si) is mostly of longitudinal character. Figures 5(c) and 5(d) correspond to the modes respectively labeled 3 and 4 in Fig. 3(b) with velocities lying between C_t(Si) and C_l(Si). The mode labeled 3 in Fig. 3(b) ($C=6.609$ km/s) shows a strong localization in the topmost GaAs layer [see Fig. 5(c)] and, therefore, is confined in the latter even though the shear component of this wave is traveling in the Si buffer layer. The mode labeled 4 in Fig. 3(b) is propagating in the two adsorbed layers with a pronounced amplitude of the transverse component in the Si buffer layer, while the longitudinal partial wave is evanescent in the latter as its velocity ($C=7.032$ km/s) lies below C_l(Si). The mode labeled 5 in Fig. 3(b) shows, as predicted, a propagation of the acoustic wave in the whole GaAs/Si/GaAs system [Fig. 5(e)] as its velocity ($C=9.335$ km/s) lies above C_l(Si). Figures 5(a), 5(b), and 5(c) evidence what we believe is one of the main outcomes of this work, namely, the existence of well-confined modes in the topmost GaAs layer even though they are in resonance with the bulk modes of the GaAs substrate. Figures 5(d) and 5(e) have been presented for the sake of completeness but the corresponding peaks are probably very weak to be observable experimentally.

As mentioned above, the pseudomodes induced by the bilayer are dependent on the width of the buffer layer. Figure 6 illustrates the variation of the velocity of the pseudomodes as a function of the thickness ratio d_1/d_2, for a given value of the surface layer thickness d_2 such that $k_{\parallel}d_2=10$. Besides the Rayleigh branch, the next branches below C_t(Si) and a few branches between C_t(Si) and C_l(Si) are almost horizontal, which means that the velocities of the corresponding pseudomodes are independent of the thickness d_1 of the Si

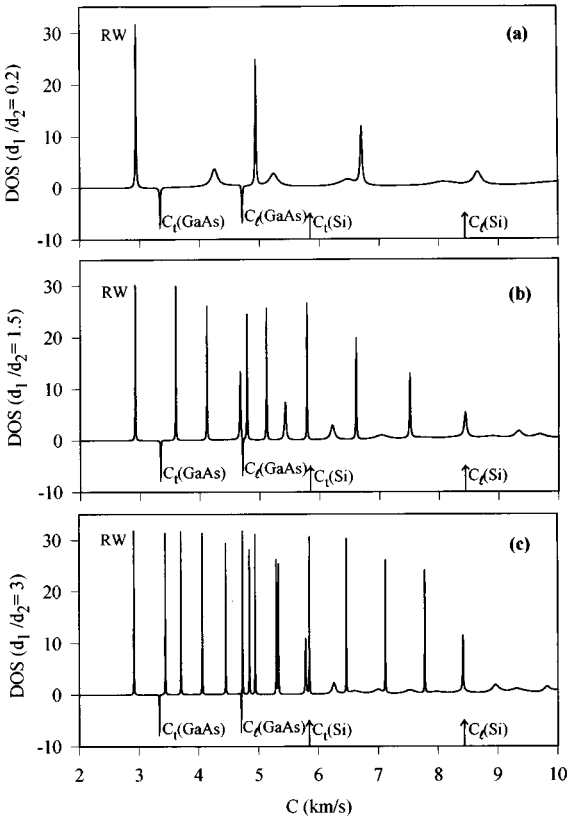

FIG. 7. Variation of the DOS due to the adsorption of the GaAs-Si bilayer on the GaAs substrate for $k_{\parallel}d_2=10$ and different values of d_1/d_2: 0.2 (a), 1.5 (b), 3 (c).

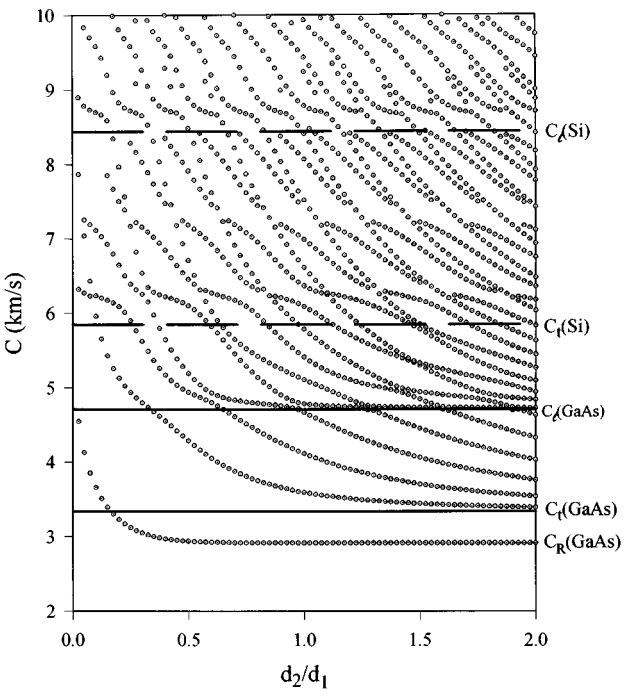

FIG. 8. Variation of the velocity of the resonant modes, for $k_{\parallel}d_1=10$, as a function of d_2/d_1.

buffer layer; these pseudomodes, which are essentially guided modes of the topmost GaAs layer, appear in general as very sharp peaks in the DOS (illustrated in Fig. 7), except for small values of d_1 [Fig. 7(a)] where the phonons in the surface layer may keep an important interaction with those in the substrate. In the velocity range between C_t(Si) and C_l(Si) there also exist dispersive branches in Fig. 6 that go asymptotically to C_t(Si) for increasing values of d_1. The latter pseudomodes actually correspond to small peaks of the DOS (Fig. 7) and are associated with a resonant behavior inside the Si buffer layer or in both surface layers. At the crossings of the flat and dispersive branches in Fig. 6, the peaks in the DOS broaden and become rather small. Finally in the velocity range above C_l(Si) the peaks in the DOS remain always very small (see Fig. 7).

In the same manner, we have studied the behavior of the resonant modes as a function of the surface GaAs layer thickness. Figure 8 presents the variation of the velocity of the resonances as a function of the ratio d_2/d_1, for a given value of the buffer layer thickness d_1 such that $k_{\|}d_1=10$. Except the lowest branch associated with the Rayleigh wave, the next branches are all dispersive and go asymptotically to the limit of C_t(GaAs) for an increasing value of d_2. One can observe coupling and anticrossing between the branches in the vicinity of C_l(GaAs) as well as in the velocity range from C_l(GaAs) to the C_t(Si). Between C_t(Si) and C_l(Si), we obtained guided resonant modes in the adsorbed bilayer with an important coupling of these pseudomodes at the crossing points. In addition there are no flat branches associated with guided modes of the Si buffer layer because the velocities of sound in Si are higher than those of GaAs. To emphasize the guided modes of the buried layer, its velocities of sound have to be chosen lower than those of the topmost layer and of the substrate; this requirement is, for example, achieved in the case of a Si-SiO_2 bilayer on a Si substrate.[19,20]

IV. CONCLUSION

The results presented in this paper are based on an analytical calculation of the response functions for acoustic waves of sagittal polarization in an adsorbed bilayer.[28] These complete response functions can be used to study any physical property of the adsorbed bilayer.[29] These include the calculation of local and total densities of states and the determination of the dispersion relation for surface guided waves in this structure. Of course, the Green's-function approach used in this analysis also enables us to obtain the displacement field associated with multiple reflection and transmission at the different interfaces, even though we do not emphasize this aspect here.

The expressions of the DOS enable us to derive the dispersion of localized and resonant modes (called also leaky or pseudowaves) in the adsorbed bilayer. Particular attention was devoted to sharp guided resonant waves confined in the topmost layer, as a consequence of its separation from the substrate by the buffer layer, when the velocities of sound in the buffer are higher than those in the topmost layer. These resonances appear as well-defined peaks of the DOS, with their relative importance being very dependent on the wave vector $k_{\|}$ and the thicknesses of the buffer and topmost layers as well as on the parameters of the constituents. Although in our illustrations (Figs. 2, 6, and 8) most of these resonances were situated below the buffer bulk band, the opposite situation can also be realized by interchanging the two constituent materials.[19,20] The experimental observation of the sharp resonances in an adsorbed slab predicted here can be possible with Brillouin scattering.[13,19,20]

*Author to whom correspondence should be addressed.

[1] A. E. H. Love, *Some Problems of Geodynamics* (Cambridge University Press, London, 1911).

[2] K. Sezawa and K. Kanai, Bull. Earth. Res. Inst. Univ. Tokyo **13**, 237 (1933).

[3] G. W. Farnell and E. L. Adler, *Physical Acoustics Principles and Methods*, edited by W. P. Mason and R. N. Thurston (Academic, New York, 1972), Vol. 9, p. 35; B. A. Auld, *Acoustic Fields and Waves in Solids* (Wiley, New York, 1973), Vols. I and II.

[4] J. A. Bell, R. J. Zanoni, C. T. Seaton, G. I. Stegeman, W. R. Bennett, and C. M. Falco, Appl. Phys. Lett. **51**, 652 (1987).

[5] J. A. Bell, W. R. Bennett, R. Zanoni, G. I. Stegeman, C. M. Falco, and F. Nizzoli, Phys. Rev. B **35**, 4127 (1987).

[6] J. A. Bell, W. R. Bennett, R. Zanoni, G. I. Stegeman, C. M. Falco, and C. T. Seaton, Solid State Commun. **64**, 1339 (1987).

[7] P. Baumgart, B. Hillebrands, R. Mock, G. Güntherodt, A. Boufelfel, and C. M. Falco, Phys. Rev. B **34**, 9004 (1986).

[8] P. Bisanti, M. B. Brodsky, G. P. Felcher, M. Grimsditch, and L. R. Sill, Phys. Rev. B **35**, 7813 (1987).

[9] G. Carlotti, D. Fioretto, L. Giovannini, G. Socini, V. Pelosin, and B. Rodmacq, Solid State Commun. **81**, 487 (1992).

[10] E. H. El Boudouti and B. Djafari-Rouhani, Phys. Rev. B **49**, 4586 (1994).

[11] G. Benedek, J. Ellis, A. Reichmuth, P. Ruggerone, H. Schief, and J. P. Toennies, Phys. Rev. Lett. **69**, 2951 (1992).

[12] C. E. Bottani, G. Ghislotti, and P. Mutti, J. Phys. Condens. Matter **6**, L85 (1994); G. Ghislotti and C. E. Bottani, Phys. Rev. B **50**, 12 131 (1994).

[13] R. J. Van Wijk, A. F. M. Arts, and H. W. de Wijn, J. Appl. Phys. **74**, 2475 (1993).

[14] B. Hillebrands, S. Lee, G. I. Stegman, H. Cheng, J. E. Potts, and F. Nizzoli, Phys. Rev. Lett. **60**, 832 (1988); Surf. Sci **211/212**, 387 (1989); S. Lee, B. Hillebrands, G. I. Stegman, H. Cheng, J. E. Potts, and F. Nizzoli, J. Appl. Phys. **63**, 1914 (1988).

[15] F. Nizzoli, B. Hillebrands, S. Lee, G. I. Stegman, G. Duda, G. Wegner, and W. Knoll, Phys. Rev. B **40**, 3323 (1989).

[16] V. Bortolani, A. M. Marvin, F. Nizzoli, and G. Santoro, J. Phys. C **16**, 1755 (1983).

[17] G. Carlotti, D. Fioretto, G. Socino, and E. Verona, J. Phys. Condens. Matter **7**, 9147 (1995).

[18] A. Akjouj, E. H. El Boudouti, B. Djafari-Rouhani, and L. Dobrzynski, J. Phys. Condens. Matter **6**, 1089 (1994).

[19] F. Nizzoli, C. Byllos, L. Giovannini, C. E Bottani, G. Ghislotti, and P. Mutti, Phys. Rev. B **50**, 2027 (1994).

[20] C. Byloos, L. Giovannini, and F. Nizzoli, Phys. Rev. B **51**, 9867 (1995); G. Ghislotti, C. E. Bottani, P. Mutti, C. Byloos, L. Giovannini, and F. Nizzoli, *ibid.* **51**, 9875 (1995).

[21] J. A. Bell, R. Zanoni, C. T. Seaton, G. I. Stegman, J. Makous, and C. M. Falco, Appl. Phys. Lett. **52**, 610 (1988).

[22] Z. P. Guan, X. W. Fan, H. Xia, S. S. Jiang, and X. K. Zhang, J. Appl. Phys. **76**, 7619 (1994).

[23] L. Dobrzynski, Surf. Sci. Rep. **11**, 139 (1990), and references therein.

[24] L. Dobrzynski, J. Mendialdua, A. Rodriguez, S. Bolibo, and M. More, J. Phys. (Paris) **50**, 2563 (1989).

[25] F. Garcia Moliner and V. R. Velasco, *Theory of Single and Multiple Interfaces. The Method of Surface Green Function Matching* (World Scientific, Singapore, 1992); B. Djafari-Rouhani and E. M. Khourdifi, in *Light Scattering in Semiconductor Structures and Superlattices*, edited by D. J. Lockwood and J. F. Young (Plenum, New York, 1991), p. 139.

[26] B. Djafari-Rouhani, A. Khelif, E. H. El Boudouti, A. Akjouj, and L. Dobrzynski, Acta Phys. Pol. A **89**, 129 (1996).

[27] A. Akjouj, E. H. El Boudouti, B. Sylla, B. Djafari-Rouhani, and L. Dobrzynski, Solid State Commun. **97**, 611 (1996).

[28] E. H. El Boudouti, B. Djafari-Rouhani, and A. Akjouj (unpublished).

[29] M. G. Cottam and A. A. Maradudin, in *Surface Excitations, Modern Problems in Condensed Matter Sciences*, edited by V. M. Agranovich and R. Loudon (North-Holland, Amsterdam, 1984), Vol. 9, p. 5.